

Chapter – 5

Chapter 5

PALEOSEISMIC AND ACTIVE FAULT STUDIES

INTRODUCTION

Seismically Kachchh region is highly hazardous, being the only region in Peninsular India placed in zone V (high seismicity) of Seismic Zoning Map of India. The region has experienced earthquakes with magnitude greater than 7 within span of 182 years. Except for 1819 Allah Bund earthquake none of the historically recorded seismic events have exhibited surface rupture in the region of Kachchh. This makes paleoseismic investigation more complex and challenging in the region.

It has been observed that maximum earthquakes that occurred in historic past in Kachchh are confined along Allah Bund Fault, Kachchh Mainland Fault and Katrol Hill Fault (Malik et al., 1999). A summary of earthquake events that have occurred in Kachchh region since 1668 to 2008 is given in table-5.1 (events up to 1996 have been listed by Malik et al. 1999).

Table 5.1: LIST OF HISTORICAL (NON-INSTRUMENTAL) AND MORDERN (INSTRUMENTAL) SEISMICITY IN KACHCHH, WESTERN INDIA FROM 1668 TO 2008.

Sr. no.	Date	Latitude	Longitude	Location	Magnitude	Source
1	6-5-1668	25.00	68.00	Indus delta	7.8	a, b, e, f
2	16-6-1819	24.16	69.16	Allah Bund	8.3	b, e
3	27-1-1820	23.42	69.90	Bhuj	3.7	E
4	13-11-1820	23.42	69.80	Bhuj	3.7	E
5	13-8-1821	23.17	70.17	Anjar	5	a, e
6	20-7-1828	23.33	69.90	Kachchh	4.3	E
7	1844	23.80	68.90	Lakhpat	4.3	E
8	19-4-1845	23.80	68.90	Lakhpat	6	e
9	19-6-1845	23.80	68.90	Lakhpat	6.3	E

Sr. no.	Date	Latitude	Longitude	Location	Magnitude	Source
10	25-4-1845	24.00	69.00	Sindri Lake, Allah Bund	6	a, e, d
11	2-11-1856	23.20	69.90	Anjar	3.5	C
12	29-4-1864	24.00	70.00	Nagar Parkar	5	D
13	10-6-1882	23.30	70.42	Bhachau	5	D
14	28-6-1882	23.35	70.58	Lakadia	5	E
15	29-6-1882	23.33	70.42	Bhachau	5	C
16	15-12-1882	23.33	70.42	Bhachau	3.5	D
17	20-8-1888	23.83	70.00	Khavda	3.5	D
18	1-6-1890	23.42	68.67	Lakhpat	4	D
19	11-1-1892	23.83	70.00	Khavda	3.5	D
20	9-7-1892	23.50	70.72	Banni	3.5	D
21	4-11-1893	23.83	68.83	Lakhpat	3.5	D
22	26-2-1896	23.83	69.67	Khavda	3.5	D
23	30-1-1898	23.16	70.08	Bhachau	3.5	D
24	1-4-1898	23.33	70.13	Bhachau	4	D
25	13-9-1898	23.55	70.42	Bhachau	4	D
26	15-10-1898	23.17	70.17	Bhachau	4	D
27	21-12-1900	23.55	70.42	Bhachau	3.5	D
28	14-1-1903	24.00	70.00	Great Rann	6	e, d
29	9-4-1904	23.33	69.67	Bhuj	4	D
30	28-4-1904	23.50	70.16	Bhachau	4	D
31	30-7-1904	23.83	70.33	Khadir	3.5	D
32	30-11-1904	24.33	69.58	Khavda	3.5	D
33	10-7-1905	23.33	69.67	Bhuj	3.5	D
34	11-1-1906	23.83	70.33	Khadir	3.5	D
35	30-6-1906	23.83	69.75	Khavda	3.5	D
36	12-3-1907	23.83	69.75	Khavda	3.5	D
37	12-7-1907	22.91	69.83	Mundra	3.5	D
38	9-10-1907	23.83	69.75	Khavda	3.5	d

Sr. no.	Date	Latitude	Longitude	Location	Magnitude	Source
39	21-10-1907	23.25	70.33	Bhachau	3.5	D
40	29-9-1908	23.83	69.75	Khavda	3.5	D
41	21-10-1908	23.83	69.75	Khavda	3.5	D
42	7-2-1909	23.83	69.75	Khavda	3.5	D
43	9-4-1909	23.25	70.33	Bhachau	3.5	D
44	24-3-1910	23.25	69.75	Bhuj	3.5	C
45	1-8-1910	23.83	69.67	Khavda	3.5	D
46	13-12-1910	23.25	70.33	Bhachau	4	D
47	16-12-1910	23.25	70.33	Bhachau	3.5	d, c
48	23-1-1911	23.41	70.58	Bhachau	3.5	d, c
49	11-10-1911	24.33	69.50	Allah Bund	3.5	D
50	1-10-1912	23.83	69.75	Khavda	3.5	D
51	7-11-1912	23.83	70.33	Khadir	3.5	D
52	26-6-1913	23.75	69.75	North Wagad	3.5	D
53	10-6-1918	23.50	70.41	North Wagad	3.5	D
54	18-10-1920	23.50	70.75	North Wagad	3.5	D
55	13-11-1920	23.33	69.67	Bhuj	3.5	D
56	11-2-1921	25.00	70.70	Nagar Parkar	4.2	C
57	26-10-1921	25.00	68.00	Indus delta	5.5	e, d
58	27-10-1921	23.42	69.67	Bhuj	4	D
59	9-2-1922	23.41	70.67	Bhachau	3.5	D
60	13-3-1922	23.41	69.37	Bhuj	3.5	D
61	7-8-1923	22.91	69.45	Mandvi	4	D
62	5-3-1924	23.91	69.83	Kaladongar	3.5	D
63	25-10-1924	23.67	68.91	Khavda	3.5	D
64	1-10-1925	23.83	69.67	Khavda	3.5	D
65	13-10-1925	23.33	70.28	Bhachau	3.5	D
66	26-12-1926	23.91	69.70	Khavda	3.5	D
67	18-11-1927	23.58	70.42	Bhachau	3.5	D
68	30-12-1930	23.91	69.45	Khavda	3.5	D

Sr. no.	Date	Latitude	Longitude	Location	Magnitude	Source
69	6-3-1932	23.83	70.33	Khadir	3.5	d
70	25-1-1935	23.58	70.67	Rapar	3.5	D
71	23-7-1935	23.25	69.50	Bhuj	3.5	D
72	31-10-1940	23.70	69.90	Banni	6	E
73	13-11-1940	23.57	70.33	Anjar	4	d, c
74	30-1-1941	23.83	70.25	Khadir	3	D
75	14-6-1950	24.00	71.20	Great Rann	5.3	C
76	21-7-1956	23.30	70.00	Anjar	6.1	d, e, f
77	22-7-1956	23.16	70.00	Anjar	3.5	D
78	12-3-1962	24.10	70.90	Great Rann	4	e, d
79	13-7-1963	24.90	70.30	Great Rann	5.3	C
80	26-3-1965	24.30	70.00	Great Rann	5.3	E
81	27-5-1966	24.46	68.69	Nagar Parkar	5	A
82	12-11-1966	25.12	68.04	Karachi	4.8	C
83	23-3-1969	24.40	68.70	Allah Bund	4.4	E
84	13-2-1970	24.60	68.61	Allah Bund	5.2	C
85	14-5-1971	25.12	68.11	Thar, Pakistan	4.5	C
86	5-6-1973	25.09	68.07	Thar, Pakistan	4.8	C
87	19-9-1975	24.69	71.03	Nagar Parkar	3.7	C
88	4-6-1976	24.51	68.45	Allah Band, Pakistan	5.1	d, c
89	26-9-1977	25.38	68.24	Karachi	4.5	C
90	21-7-1980	22.87	72.14	Nartrang	3.1	C
91	26-4-1981	24.12	69.51	Allah Bund	4.3	C
92	31-1-1982	24.21	69.84	Great Rann	4.8	C
93	18-7-1982	23.40	70.66	North Wagad	4.8	C
94	13-9-1984	24.95	70.46	Allah Band, Pakistan	4.2	C
95	7-4-1985	24.36	69.74	Great Rann	5	d, c
96	10-2-1987	24.10	70.39	Great Rann	3.9	C

Sr. no.	Date	Latitude	Longitude	Location	Magnitude	Source
97	10-4-1987	24.55	70.12	Great Rann	2	C
98	17-7-1988	25.16	70.00	Thar, Pakistan	2	d
99	21-3-1989	24.27	68.96	Allah Bund	4	C
100	10-12-1989	24.81	70.88	Lunu delta	4.7	C
101	20-1-1991	23.13	69.83	Anjar	2	D
102	20-1-1991	23.40	69.71	Anjar	4.9	C
103	10-9-1991	24.16	68.68	Allah Bund	4.7	C
104	10-9-1991	24.28	68.80	Nagar Parkar	4.7	C
105	4-5-1992	24.52	70.13	Nagar Parkar	3.5	d, c
106	9-2-1993	24.62	68.93	Nagar Parkar	4.3	C
107	17-2-1996	23.33	69.67	Bhuj	4.5	D
108	5-8-1996	22.83	68.43	Bhuj	3.8	C
109	8-10-1998	24.45	69.80	Nagar Parkar	3.7	C
110	24-12-2000	24.01	70.09	Great Rann	4.7	C
111	26-1-2001	23.44	70.31	North Wagad	7.7	
112	3-2-2006	23.92	70.44	Gedi, Rapar	5	C
113	7-3-2006	23.79	70.73	Gedi, Rapar	5.7	C
114	6-4-2006	23.78	70.74	Gedi, Rapar	4.8	C
115	6-4-2006	23.34	70.39	Lakadia, Bhachau	5.6	C
116	10-4-2006	23.51	70.06	Kachchh	4.9	C
117	9-3-2008	23.39	70.33	Chobari, Bhachau	4.9	C

Data source:

- (a) India Meteorological Department, New Delhi.
- (b) Bilham (1999).
- (c) Annual Report (2006-07), Institute of Seismological Research (ISR), Gandhinagar.
- (d) Malik et al. (1999).
- (e) USGS, National Earthquake Information Centre.
- (f) Chung and Gao, (1995).

Landscape of Kachchh provides good example of terrain with active tectonic control (Malik et. al. 2001). The Ranns of Kachchh and Banni plains furnish suitable conditions for occurrence and preservation of seismically induced soft sediment deformation and liquefaction features (Fig. 5.1). Region has congenial geomorphic setting for existence of active tectonic geomorphic markers, e.g. Northern Hill Range brought up by Kachchh Mainland Fault provides suitable geomorphic setting for unconfinement of north flowing streams originating from Kachchh Mainland. Alluvial fans, produced by these streams in Great Rann-Banni depression after crossing Northern Hill Range and eventually Kachchh Mainland Fault are found to be uplifted and incised by same rivers (Malik et. al. 2001). This asserts active tectonic influence in the region.



Fig. 5.1: Liquefaction crater seen in epicentral area of 2001 Bhuj earthquake.

BACK GROUND OF PALEOSEISMIC AND ACTIVE FAULT STUDIES IN KACHCHH

Spectacular geomorphic changes caused by 1819 Allah Bund earthquake in Rann of Kachchh have attracted many workers to study paleoseismic aspects of Kachchh (Burnes 1833, Grant 1837, Baker 1844, Lyell 1850, Wynne 1872, Oldham 1898, Sivewright 1907, Reid 1911, Oldham 1926, Malik et al. 1999, Bilham 1999, Rajendran & Rajendran 2001). Attempts are made to decipher rupture geometries of 1819 Allah Bund earthquake (Bilham 1999, Rajendran & Rajendran 2001). Although seismic history of region (table 5.1) indicates that the region is characterised by number of active faults; studies to identify and evaluate active faults in region are fewer (Malik et al. 2001, Mathew et al. 2006, Karanth and Gadhavi, 2007, Malik et al. 2008, Morino et al. 2008a, Morino et al. 2008b).

First ever attempt to traces active faults in the pediment zones along the northern margins of Katrol Hill Range and Northern Hill Range was made by Malik et al. 2001. By satellite photo interpretation they observed that active faults have displaced along them Late Quaternary alluvial fan deposits and colluvial debris. Scattered traces of active faults were identified along the pediment zone of Northern Hill Range, where uplift was observed along north facing scarplets. Similarly along Katrol Hill Range active tectonic features were identified aligned with old Mesozoic structures, manifested by straight linear ridges and linear contact between the rocky outcrop and alluvium in foreground.

To confirm active faulting along the Kachchh Mainland Fault first ever trench studies were carried out by Malik et al. 2008a near Lodai village to the west of Kaswali River fan. At the base of 3 m to 4 m high fault scarp 15 m long, 3.5 m wide and 2 m deep trench was excavated. Three major fault strands dipping 10° to 55° due south were

identified, wherein, fault strand placed foreland ward (leading strand) was observed to be gently dipping and trailing fault strands were observed progressively steeper. Older Mesozoic rocks were observed placed over younger Quaternary deposits along steep trailing fault. Based on stratigraphic cross cutting relationship two events were identified along leading fault.

Based on satellite photo interpretation and field survey Morino et al. 2008a identified several possible traces of active fault along Katrol Hill Fault (KHF) as well. They also proposed existence of a new active fault named as Bhuj Fault that extends into the Bhuj Plain. Active fault traces were recognized about 1 km north of the topographic boundary between the Katrol Hill and the Bhuj plain. Trenches were excavated to identify the paleoseismic events, pattern of faulting and the nature of deformation. The fault exposure along the west bank of Khari River with 10 m wide shear zone in the Mesozoic rocks exhibiting displacement of the overlying Quaternary deposits was observed. They observed that E-W trending discontinues active fault traces along the Katrol Hill Fault in the western part changes to NE-SW or ENE-WSW to follow Bhuj Fault. Trenching survey across a low scarp revealed three major fault strands along which three large magnitude earthquake events were recognised.

ACTIVE FAULT STUDIES ALONG KACHCHH MAINLAND FAULT

During present study of trench investigation were carried out along Kachchh Mainland Fault near Jhura village and Khirsara village (Fig. 5.2). (This study was carried out during author's tenure at Institute of Seismological Research, Gandhinagar in collaboration with OYO International Corporation, Japan and Indian Institute of Technology, Kanpur; the study was funded by Gujarat State Disaster Management Authority (GSDMA), Gujarat, India.)

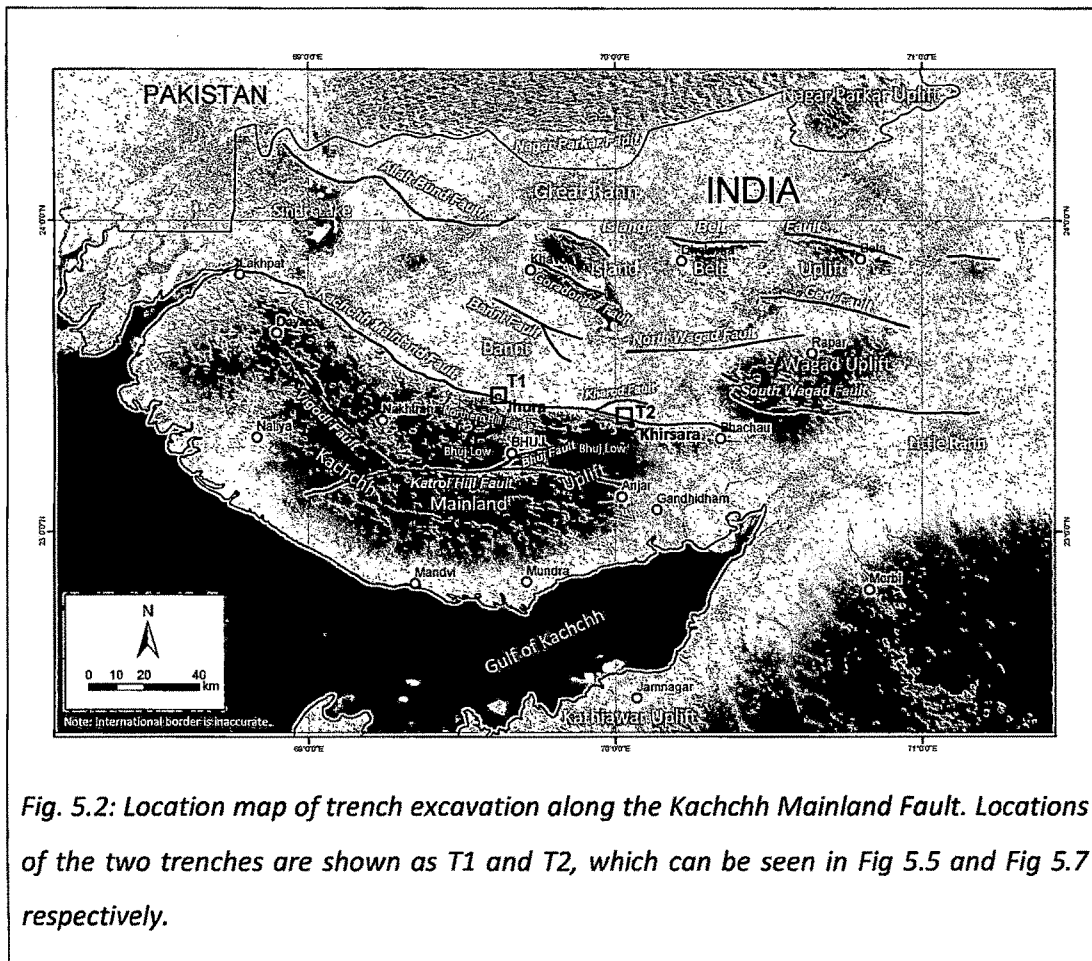


Fig. 5.2: Location map of trench excavation along the Kachchh Mainland Fault. Locations of the two trenches are shown as T1 and T2, which can be seen in Fig 5.5 and Fig 5.7 respectively.

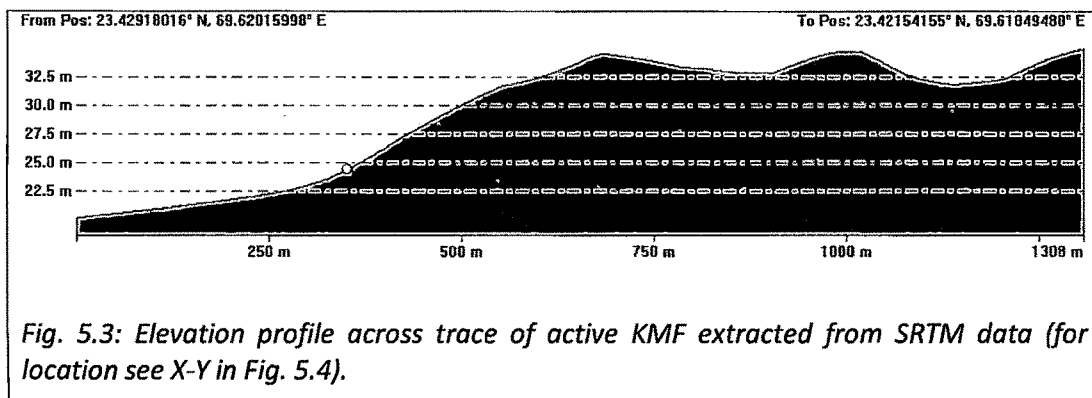
Trench investigation along Kachchh Mainland Fault near Jhura village revealed active fault, displacing alluvial fan deposits of Kaila River (Fig. 5.2). Two fault strands F1 and F2 were identified in the trench. The northern fault F1 shows a low-angle reverse fault with inclination of 15° toward south. Three seismic events were inferred in the trench from upward fault termination with clear angular unconformities. The net-slip for single event considering deformation on the hanging wall of F1 fault is proposed to be ≈ 5 m (Morino et. al. 2008b).

Only one active fault strand was observed in a trench near Khirsara village. In the trench along the western wall it was observed that Quaternary units are displaced by 30

cm to 56 cm along a south dipping fault. However, rupture along eastern wall was not well defined.

Trench investigation near Jhura– Trench T1

Traces of active faults in pediment zone northern side of Kachchh Mainland Fault were identified from the CORONA satellite photo interpretation and field survey. CORONA satellite photo around Jhura village and topographic profile extracted from SRTM data (Fig. 5.3) revealed uplifted flat surface at the base of Jhurio Hills.



From satellite data as well as during field survey it was observed that active uplift has resulted in formation of about 5 m high NNE facing low scarp demarcating the topographic boundary between the northern alluvial fan of Kaila River and southern uplifted flat surface (Fig. 5.3). The southwestern uplifted terrace has been incised by many small channels. Evidences of displacement along Kachchh Mainland Fault was observed to the south of low scarp at the contact between highly sheared Jurassic shale and Tertiary conglomerate (Fig. 5.4)

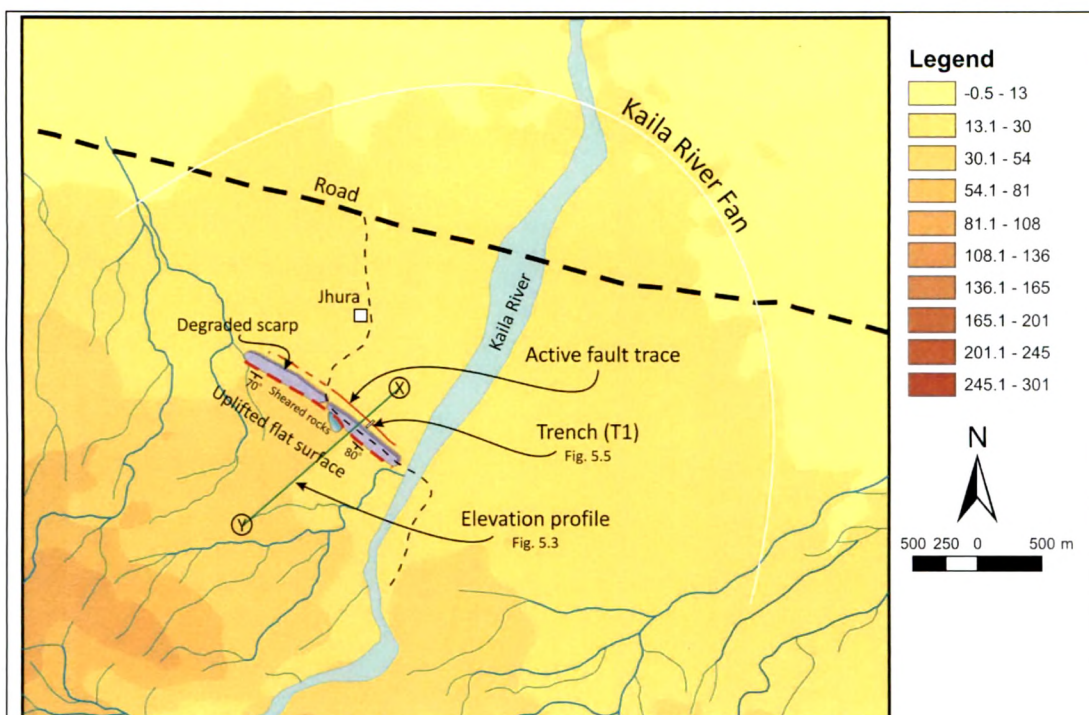


Fig. 5.4: Morphology around Jhura Trench (T1), uplifted fan deposits were observed to the south of NW-SE striking degraded scarp, X-Y indicate end-points of elevation profile (Fig. 5.3), See Fig. 5.2 for location.

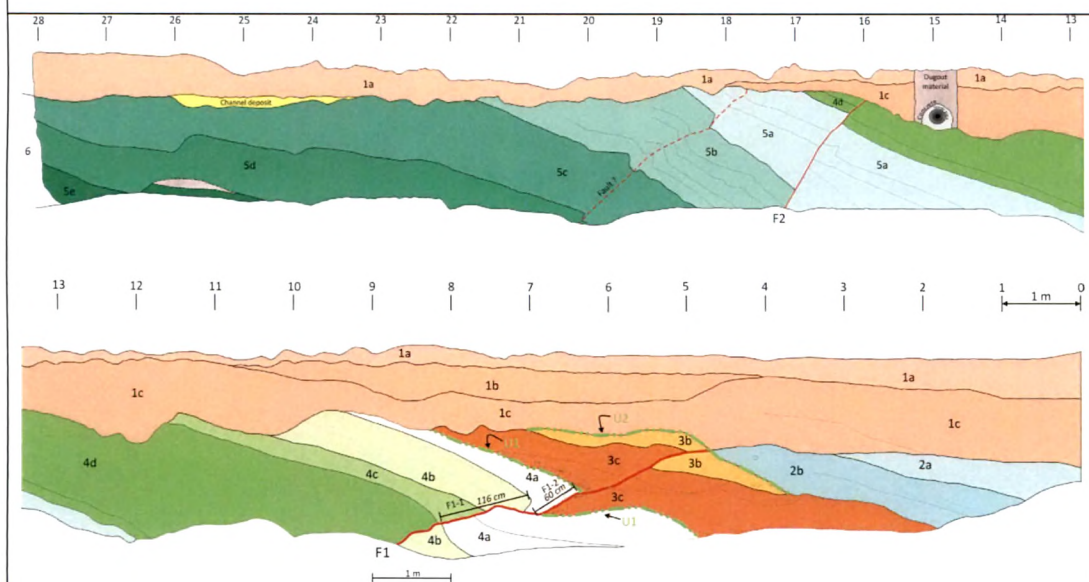


Fig. 5.5: Trench log of western wall of Trench T1 excavated near Jhura village across trace of active KMF.

This study was carried out during author's tenure at Institute of Seismological Research, Gandhinagar in collaboration with OYO International Corporation, Japan and Indian Institute of Technology, Kanpur; the study was funded by Gujarat State Disaster Management Authority (GSDMA), Gujarat, India.)

Stratigraphy of Trench-1

Several units of medium to coarse sand and fine gravel representing channelized over-bank deposits of alluvial fan aggraded by Kaila river fan were observed in 28 m long, 2 m wide and 2.5 m deep trench (Fig. 5.5) excavated at the geomorphic boundary (Fig. 5.4). The succession is marked by typical upward fining sequence with gravel or coarse sand at the base and medium to fine sand in the upper part. Based on the repetitive sequence and angular unconformity with respect to the faulting, the exposed sedimentary succession was divided into 6 units (1 to 6). Units 1 to 5 were further divided into sub-units like a, b, c, d (Morino et al. 2008b).

Poorly stratified medium to coarse sand with gravel at the base comprises Unit 1. Since this unit overlies all the units exposed in the trench, it is suggested to be deposited by the present channel. Subunit 1b is a channel deposit forming lens of sand and gravel. Unit 2 is subdivided into Subunits 2a to 2c, where Subunit 2a consists of massive fine sand, 2b is made up of stratified fine sand, and 2c consists of fine sand with scattered fine gravels. However, along the west wall of the trench only Subunits 2a and 2b are preserved, Subunit 2c and underlying Subunit 3a are seen only along the east wall of the trench (see Fig. 4, 5 and 6 Morino et al. 2008b). Along the west wall Subunit 2b is seen directly overlying Subunit 3b (Fig. 5.5). This contact is marked by erosional unconformity, where significant amount of erosion has removed Subunits 2c, 3b and part of 3b along the west wall.

Unit 3 as a whole (with Subunits 3c to 3a) exhibits fining upward sequence suggesting over-bank deposit of Kaila River. These units are inclined to north with inclination of 10°-15°. The bottom of Subunit 3c is marked by angular unconformity with underlying Unit 4. The Unit 4 also exhibits upward fining sequence with medium to

coarse sand representing over-bank deposition; it is subdivided into Subunits 4a to 4d. Gravel and medium to coarse sand consists Subunit 5a; Subunit 5b is made up of massive well sorted medium sand with scattered cobbles; whereas Subunit 5c consists of poorly sorted fine to medium sand and 5d is formed of stratified medium sand.

Identification of fault strands

Extensive Quaternary deformation, associated with two prominent fault strands F1 and F2 dipping towards south, was revealed in the trench (Fig. 5.5). Fault F1 is a low-angle reverse fault with inclination of about 15°, whereas fault F2 is a relatively steep, dipping 50° due south. The youngest unit displaced by fault strand F2 is Subunit 4d. The fault dies out upward in Subunit 4d without unconformity. There exists unconformity between Subunit 4d and Subunit 5a. It appears that latest event on fault strand F2 occurred before deposition of Subunit 4d, however, some slip has occurred on fault strand F2 during the slip of younger fault strand F1, which resulted in displacement of Subunit 4d. The layers on the hanging wall of F1 fault are deformed widely, the width of the deformation is about 20 m. Looking at the large deformation associated with fault F1 it is assumed that Fault F2 is secondary fault.

The stratigraphic cross-cutting relationship suggests occurrence of two seismic events along the F1 fault. Based on stratigraphic cross-cutting relation of units and displacement variations Fault F1 is subdivided into fault strands F1-1 and F1-2. The youngest unit displaced by F1-1 strand is Subunit 4a (Fig. 5.5). The Subunit 3c capping the Subunit 4a post-dates the occurrence of this event on strands F1-1. The youngest unit displaced by northern F1-2 strand is Subunit 2c, however, along the west wall of the trench due to comparatively greater amount of erosion Subunits 2c and 3a are completely eroded along with part of Subunit 3b. These units are partially preserved

along the east wall (see Morino et al. 2008b). The eroded tip of strand F1-2 is covered by Subunit 2b. This suggests that event occurred after the deposition of Subunit 2c and before the deposition of Subunit 2b.

Deformed Quaternary units exhibit typical fault-propagation fold geometry along fault F1. Subunits 4a to 4d exhibit typical fault-propagated folding and dragging movement near the fault tip on the hanging wall of F1 strand (Fig. 5.5). This whole unit is inclined towards north with inclination of about 25° is observed on the hanging wall.

Unconformities

Two clear angular unconformities (U-1 and U-2) were observed along F1-1 and F1-2 fault strands (shown by thick green lines in Fig. 5.5; is it possible to add arrows to indicate U-1 and U-2). The first unconformity (U-1) is marked by prominent variation in inclinations between units 4 and 3. Unit 4 is dipping 25° due north whereas, overlying Units 3 is dipping 10°-15° due north. The Subunit 3c is deposited over eroded surface of Subunit 4a. This suggests that Subunit 3c was deposited after the event occurred along F1-1 strand displacing unit 4. Thus Subunit 3c and younger units were deposited after the unit 4 became inclined due to the slip of F1-1 fault strand.

Similarly, Subunits 2a and 2b covering Subunit 3b and older units mark another angular unconformity (U-2). Along the western wall of the trench Subunit 3b is directly covered by Subunit 2b, whereas along the east wall Subunit 3a and 2c are present in between (Morino et al. 2008b). Along this unconformity due to erosion tip of fault strand F1-2 is also eroded to some extent.

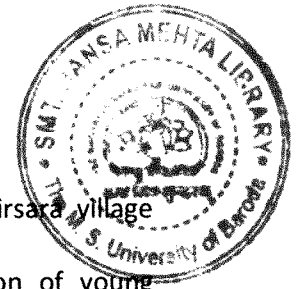
Considering the thickness variations of Subunit 4d and difference of inclination between its top and bottom it is suggested that the second angular unconformity (U-2) exists between the Subunits 4d and 5a.

Seismic events recognised in trench

Based on the stratigraphic cross-cutting relationship, variation in inclination of the units, angular unconformities and variation in displacement of units at least three seismic events; E-1, E-2 and E-3 are inferred. Units older than Subunit 4d are displaced along fault F2 indicating occurrence of one event, E-1 during the deposition of Subunit 4d. Probably, this event is responsible for tilting of Unit 5 and bottom of Subunit 4d, which is evident from angular unconformity. Movement along fault strand F1 has resulted into displacement and tilting of Unit 4 and 3. The amount of displacement for Subunit 4a is 116 cm, whereas same is 60 cm for Subunits 3c and 3b along fault F1. Moreover, Subunit 4a is covered unconformably by Subunit 3c suggesting that units older than Subunit 3c have moved twice along this fault. Thus currently measured displacement and inclination of Subunit 4a and older units is cumulative displacement of two events along fault F1. The portion of fault plane which has witnessed two events is termed here as, E-1, responsible for displacement along F1-1 and portion that has encountered only one event is termed here as, E-2, responsible for displacement along F1-2.

It is observed that Fault F1-2 is truncated at the base of Subunit 2b and it has displaced unit 3 by about 60 cm. This indicates that youngest (E-3) event has occurred before the deposition of Subunit 2b and after the deposition of Unit 3. Due to this event Unit 3 is tilted northward by about 10° to 15°.

It is also noticed that Unit 4 is displaced by fault strand F1-1 and is covered by Subunit 3c giving rise to angular unconformity, therefore, it is suggested that the penultimate seismic event occurred after the deposition of Subunit 4a and before the deposition of Subunit 3c (Fig. 5.5).



Trench investigation near Khirsara village-T2

Careful observation of drainage pattern to the north-west of Khirsara village within pediment zone of eastern Kas Hill revealed moderate disruption of young drainage along a linear narrow zone. It was observed that some of the streams have developed a sharp bend to bypass that zone; whereas others joined together to form higher order stream and to move on. From the CORONA satellite data east-west oriented low ridge was recognised along the same linear zone. During field investigation it was observed that a small pond is excavated artificially utilizing same geomorphic divide. *Presently observed artificial excavation was not at place at the time when CORONA images were collected.* Steeply north dipping to near vertical Tertiary beds characterised this low ridge. Just north of this geomorphic break, a 9 m long, 2 m wide and 2.5 m deep trench was excavated (Fig. 5.6). Along the western wall of this trench, Quaternary units were observed deformed and displaced. It was observed that Quaternary units, at different stratigraphic level, are displaced by 30 to 56 centimetres and are tilted towards north by 13° to 29° (Fig. 5.7). However, on the east wall displacement was not well defined. And therefore lateral continuity of structure observed along the western wall could not be established.

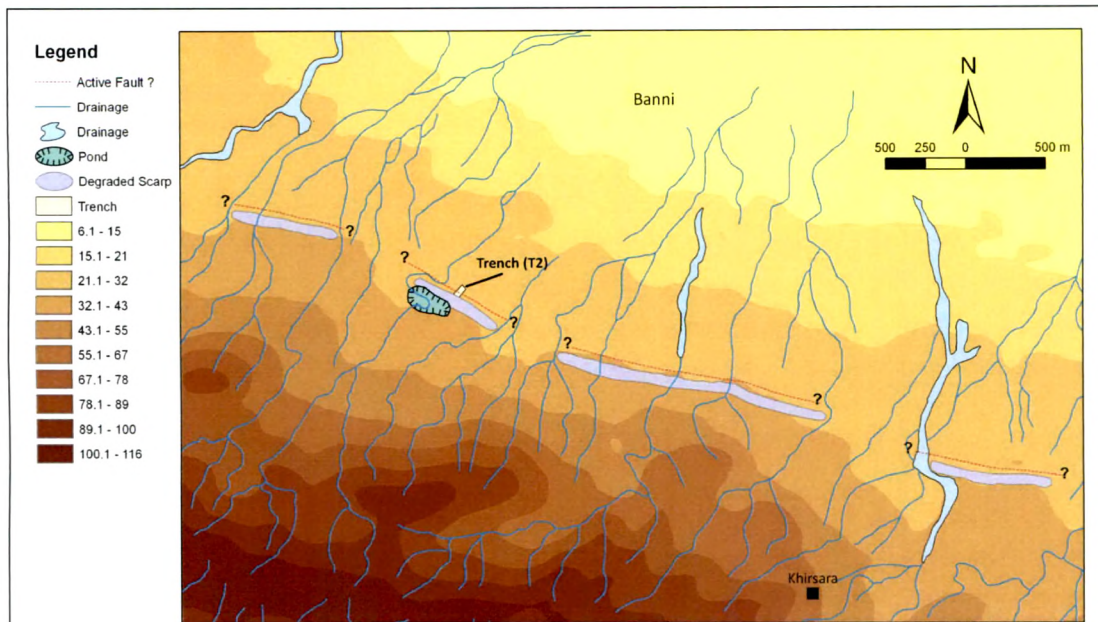


Fig. 5.6: Geomorphology around Trench T2 (Khirsara Trench).

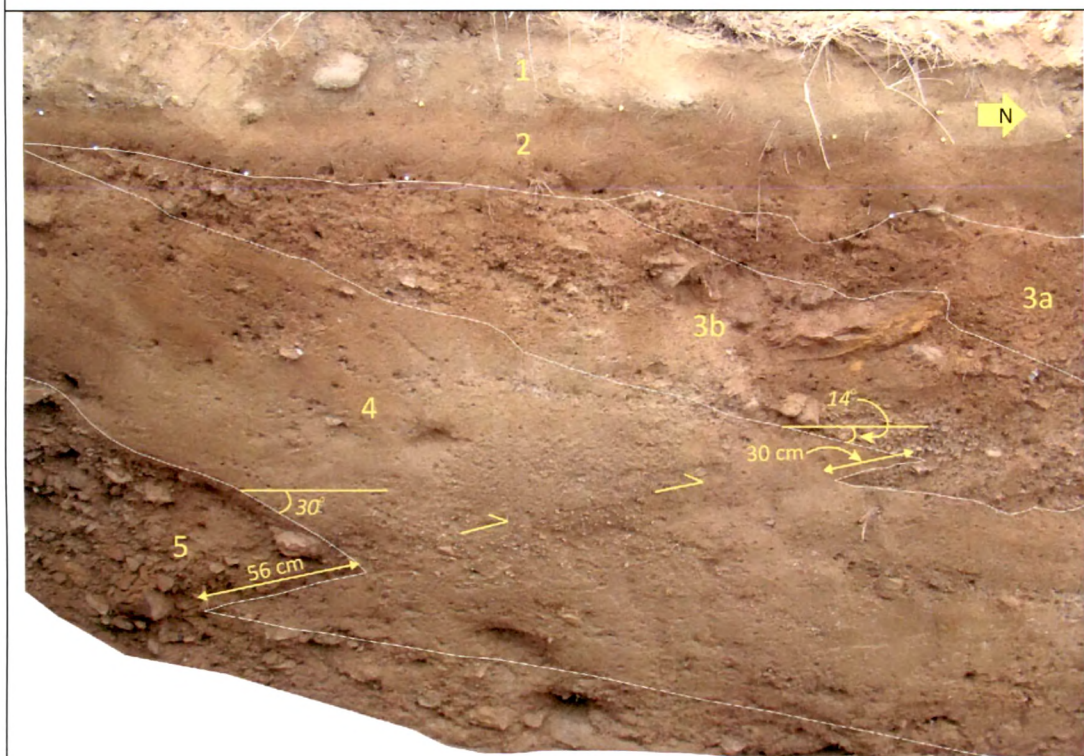


Fig. 5.7: Photograph of Khirsara Trench depicting displacement of Quaternary units.



Fig. 5.8: Photograph of Khirsara Trench depicting deformation of Quaternary units. (Arrows point to fault plane).

Stratigraphy of Trench-2

Five Quaternary units are recognised in the trench and are numbered from top to bottom as 1 to 5 (Fig. 5.7 and Fig. 5.8). The upper most Unit 1 appears to be debris washed out from artificial dyke (dam) created along the naturally formed low ridge. It consists of different sized fragments of Tertiary rocks imbedded in buff coloured clay. Below Unit 1 sub-horizontally placed reddish-brown coloured Unit 2 is recognised as soil buried under the outwash of artificial barrier. Colluvial deposits with increasing thickness towards north are recognised as Subunit 3a and Subunit 3b. Among these two units, lower Subunit 3b is displaced by about 30 cm, whereas upper Subunit 3a is observed folded but no displacement is observed. These units are observed tapered towards south close to ridge. Unit 4 consist of calcretised fine to medium sand. Owing to its thickness and diverse displacement at top and bottom Sedimentary Unit 4, which is followed by colluvial debris at the bottom of the trench numbered as Unit 5.

Quaternary deformation /Identification of fault strand

Quaternary deformation in form of folding and displacement along a low angle reverse fault was observed in the trench T2. It was observed that Unit 4 has moved 30 cm whereas, underlying Unit 5 has moved by about 56 cm. An angular unconformity is recognised between units 5 and 4, where dip of unit 4 is 14° and dip of underlying unit 5 is 30° due north (Fig. 5.7). Based on slip variation observed between unit 5 and unit 4; and angular unconformity between both the units; two events are inferred in the trench.

The trace of fault strand observed along the western wall of the trench was not well defined along the eastern wall.

ACTIVE SYNCLINAL FOLDING

Evidences of active deformation are observed from the Palara Syncline area (Fig. 4.24). Active deformation was documented from this area by previous workers (Mathew et al. 2006) as well. However, structure responsible for active deformation remained elusive. Present study demonstrates that deforming syncline, where compression induced bedding parallel slip has resulted in localised uplift and out-of-syncline thrust is responsible for localised active deformation in the area.

An assemblage of different geomorphic indicators suggesting active deformation is recognised from the area. Geomorphic features such as alluvial terraces, incised paleochannel, strath terraces, bedrock ravines, drainage reversal, aggradation and localised ponding are observed from the area (Fig. 4.24).

Alluvial terraces:

At western fringe of the syncline, active deformation is manifested by occurrence of paired alluvial terraces. Within wide Khari River valley recent valley-filled deposits are

observed incised by 3.25 m (Fig. 5.9). The age of incised deposits was estimated between 5 ka to 4 ka (Mathew et al. 2006).



Fig. 5.9: Paired valley filled alluvial terraces (shown in arrows) in Khari River. (See Fig. 4.24 for location).

Khari River that flows in approximate north direction at western border of the structure has given rise to alluvial terraces along the margin of the structure

Paleochannel

Along the incised eastern bank of Khari River, aligned to western fringe of Palara Syncline (Fig. 4.24) a hanging paleochannel (Fig. 5.10) is observed. Incision along Khari River has cut across a pre-existing channel, which had flow-direction approximately perpendicular to present day Khari River. This unique geomorphic feature, oriented almost parallel (E-W direction) to fold axis of Palara Syncline, demonstrates a sequence of incision, aggradation and incision. The paleochannel initially incised Mesozoic rock sequence and formed a ~10 m deep and ~30 m wide channel. This paleochannel

subsequently became defunct. Aggradation by valley filled deposits then occurred (Mathew et al. 2006). At later stage present day Khari River, flowing approximately perpendicular to the paleochannel, incised Mesozoic strata. In this process it also incised sediments aggraded in the paleochannel and Mesozoic strata below the base level of paleochannel by ≈ 9 m giving it appearance of hanging channel. After this stage aggradation occurred within Khari River. Again due to base level changes Khari River incised its on deposits that resulted in formation of 3.25 m high paired valley filled terraces (Fig. 5.9).

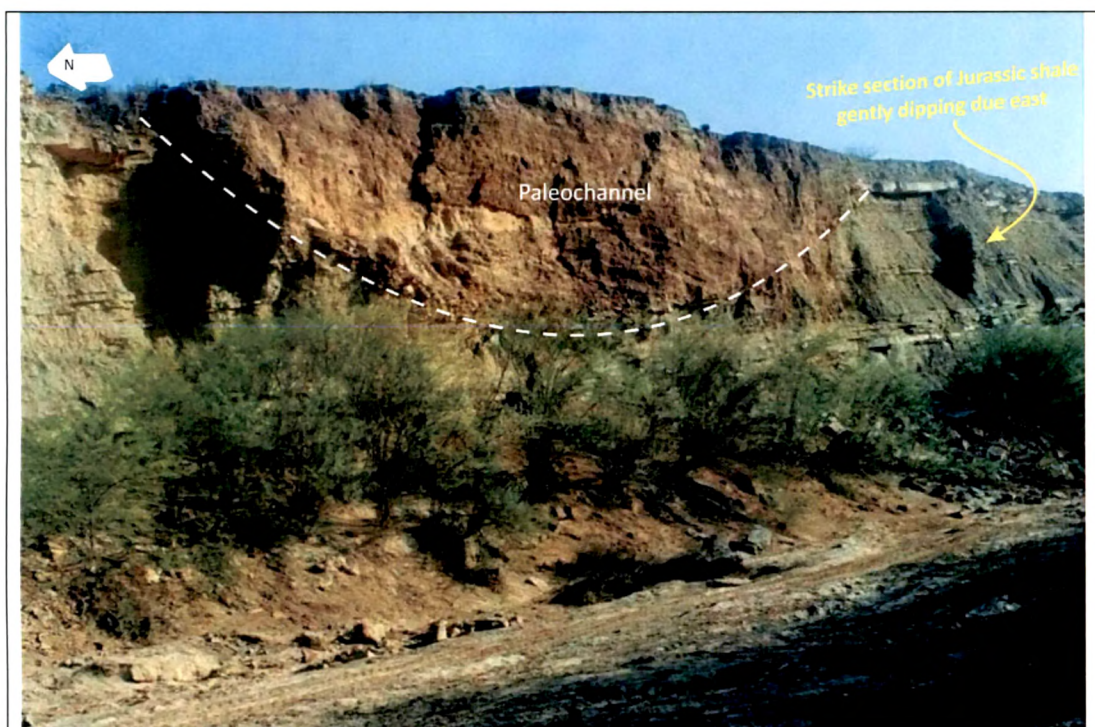


Fig. 5.10: Paleochannel observed along eastern bank of Khari River at western fringe of Palara Syncline. (see Fig. 4.24 for location).

Mathew et al. (2006) estimated OSL ages of 12.4 ± 1.6 ka for upper part of paleochannel, whereas OSL ages for paired valley filled terraces within Khari River were estimated around 5 to 4 ka.

Strath terraces

At southern side of Palara Syncline along the course of Pat River two paired strath terraces are observed (see Fig. Fig. 4.24 and Fig. 5.11). The primary surface is discerned as T_0 , two subsequent terraces are identified as T_1 and T_2 that are respectively at lower elevations. Elevation difference between T_1 and T_2 is ≈ 3.8 m (Fig. 5.11).



Fig. 5.11: Strath terraces along Pat River. (See Fig. 4.24 for location).

Strath terraces are considered to be useful local geomorphic markers (Burbank and Anderson, 2001). Tectonic perturbation results in base level change that eventually leads a drainage system from equilibrium mode to a degradational mode (Burbank and Anderson, 2001); in bedrock areas base level changes give rise to strath terraces.

Drainage reversal:

Phenomenon of drainage reversal is observed along the course of rivers Pat and Pur that flow across the actively deforming Palara Syncline. Direct response to localised flexuring is observed as water logging and aggradation.

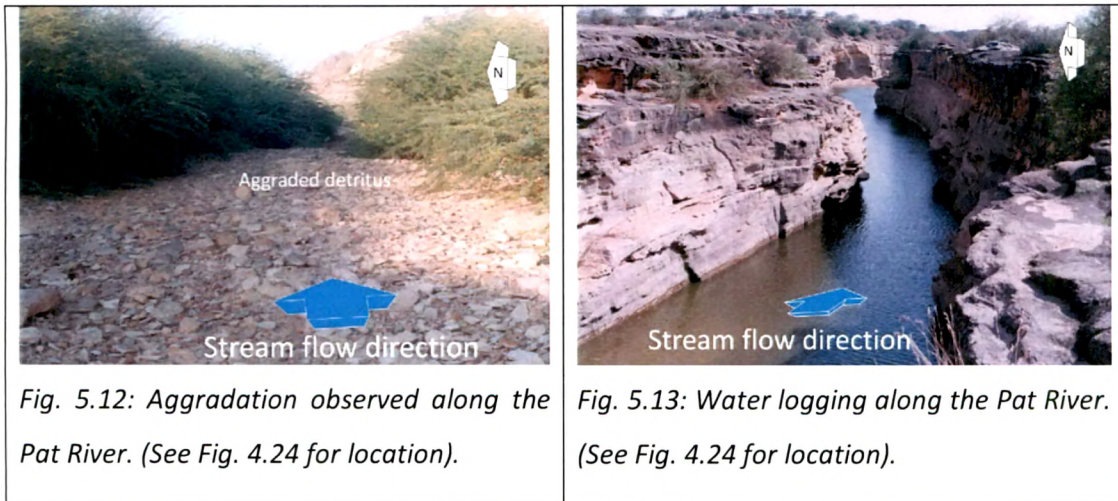


Fig. 5.12: Aggradation observed along the Pat River. (See Fig. 4.24 for location).

Fig. 5.13: Water logging along the Pat River. (See Fig. 4.24 for location).

Cobble and pebble sized angular fragments of rocks are seen spread along the course of Pat River (Fig. 5.12). These deposits are followed by water logged stream further downstream (Fig. 5.13). Along the water logged course of river on cliffy banks marks of gradually decreasing water level can be seen. From this it can be envisaged that during rainy season the level of water in the local pond along the channel was high which gradually due to evaporation and percolation has been reduced. Occurrence of detritus materials at the beginning of such ponds indicates that load carrying capacity of these seasonal streams dramatically reduces when they reach their own waterlogged course as a result whatever bed load streams carrying gets deposited at very beginning of such pond.

Bedrock incision

Narrow and deep bedrock incision is observed in a small stream that flows almost parallel to the Saraspar Thrust. The stream is situated within back limb of the thrust and it flows parallel to the structure (Fig. 5.14).



Fig. 5.14: Bedrock incision south of Saraspar Thrush. (See Fig. 4.24 for location).

Cretaceous (Bhuj Formation) sandstone is observed incised by about 30 m along a hardly 3 m wide second order stream. The orientation of the gorge is parallel to that of Saraspar Thrust (Fig. 4.24).